The EUMETSAT Network of Satellite Application Facilities

NWP SAF

Numerical Weather Prediction

Document NWPSAF-MO-TR-042

Version 1.0

NWP SAF AMV monitoring: the 10th Analysis Report (AR10)

Graeme Kelly[1], James Cotton[1], Mohamed Dahoui[2] and Mary Forsythe[1].

1. Met Office, UK

2. European Centre for Medium-Range Weather Forecasts (ECMWF)

NWP SAF AMV monitoring:10th Analysis Report (AR10)

Graeme Kelly, James Cotton, Mary Forsythe (Met Office)

Mohamed Dahoui (ECMWF)

This documentation was developed within the context of the EUMETSAT Satellite Application Facility on Numerical Weather Prediction (NWP SAF), under the Cooperation Agreement dated 7 September 2021, between EUMETSAT and the Met Office, UK, by one or more partners within the NWP SAF. The partners in the NWP SAF are the Met Office, ECMWF, DWD and Météo France.

Copyright 2023, EUMETSAT, All Rights Reserved.

Contents

1. Introduction

The NWP SAF (Satellite Application Facility for Numerical Weather Prediction) Atmospheric Motion Vector (AMV) monitoring (http://nwpsaf.eu/site/monitoring/winds- quality-evaluation/amv) provides tools to monitor, document and investigate error characteristics of AMV data.

The NWP SAF provides a long-term archive of observation-minus-background (O-B) statistics where the AMVs are compared with short-range forecasts from an NWP model. Forecast model fields are interpolated in time and space to the observation location and used to calculate a model-equivalent of the observation, referred to as the “background” value. O-B are calculated against the Met Office and ECMWF global models, to give insight into whether features seen in the monitoring are related to problems with the models or with the AMVs. Monitoring against the DWD global model will be included in the NWP-SAF archive from 2023.

Since the last NWP SAF report EUMETSAT, NOAA and JMA have rearranged their prime satellites and NOAA have made small changes in their processing software. The O-B monitoring has been an invaluable tool to validate the AMVs after satellite replacements.

An extensive set of AMV products are actively monitored by the NWP SAF (Table 1). Previous generations of satellite/instruments can also be found in the archive. New data sets added to the monitoring since 2020 are Himawari-9, Meteosat-9 (Indian Ocean Data Service (IODC)) and GOES-18 (Table 2).

Analysis reports are released at intervals of 2-years to help guide discussion on improvements to the AMV derivation and data assimilation. Results are presented at the workshops of the International Winds Working Group (IWWG). The analysis reports identify features from the monitoring statistics and document how these evolve over time. Where possible attempts are made to diagnose the cause of the difference between the AMVs and the model.

This paper marks the tenth in the series of analysis reports (AR10). Previous analysis reports are hereafter referred to by the order of their publication e.g., 9th Analysis Report (AR9), and are available to download from the NWP SAF Website.

The paper is structured as follows. Section 2 provides a status summary of the current active features in the monitoring. Section 3 explores several new datasets. Section 4 looks at some general comparisons of the O-B monitoring plots. Section 5 introduces the Nowcasting Satellite Applications Facility (NWC SAF) Nowcasting Package. Section 6 covers validity of AMV O-Bs in the African Tropical region. Section 7 provides a summary.

Geostationary AMVs	Producer	Channels
Meteosat-8/9/10/11	EUMETSAT	IR 10.8, WV 6.2, WV 7.3, VIS 0.8, HRVIS
Himawari-9	JMA	IR, WV 6.2, WV 6.7, WV 7.3, VIS
GOES-16/18	NOAA/NESDIS	IR, SWIR, WV, VIS
INSAT-3D/3DR	ISRO	IR, SWIR, WV, VIS
GK-2A	KMA	IR, SWIR, WV, VIS
FY-2G	CMA	IR, WV
Leo AMVs		
Terra	NESDIS, DB	IR
Aqua	NESDIS, DB	IR, WV, CSWV
NOAA-15/18/19	CIMSS, DB	IR
Metop-B	EUMETSAT, CIMSS	IR
Metop-C	EUMETSAT	IR
Suomi NPP	NESDIS, DB	IR
NOAA-20	NESDIS	IR
Mixed AMVs		
LeoGeo	CIMSS	IR
Dual-Metop	EUMETSAT	IR

Table 1. AMV datasets monitored by the NWP SAF. Channels are infrared (IR), short wave infrared (SWIR), visible (VIS), high resolution visible (HRVIS), cloudy water vapour (WV), clear sky water vapour (CSWV). DB stands for direct broadcast station.

Change	Type	Date available	Description
GOES-18	Transition	13 Nov 2022	GOES-18 replaced GOES-17 4 Jan 2023
Meteosat-9	Transition	12 Jul 2022	Meteosat-9 replaced Meteosat-8 12 Jul 2022 as the Indian Ocean IODC service
Himawari-9	Transition	13 Nov 2022	Himawari-9 replaced Himawari-8 13 Dec 2023
Meteosat-10	Transition	21 Mar-2023	Meteosat-10 replaced Meteosat-11 at 0 Degrees East on 21 Mar 2023

Table 2. Changes to the monitoring since AR9 (2020).

2. Index of features identified in the monitoring

Table 3 documents the features that were active from AR9 and provides an update on their status within the monitoring. In some cases, features may have been renamed from previous reports to better reflect the pattern or cause. For each feature, the table indicates whether further details are provided in the following sections of this report. A new feature investigated in AR10 is Feature 10.1: Problems in regions of organized convection in the tropics.

Features are referenced in the format X.Y, where X is the number of the analysis report where that feature was first described, and Y is the example number

Unless otherwise specified, the tropics refer to the area 20°N-20°S and the extra-tropics polewards of these boundaries. Upper-level, mid-level and low-level refer to AMV heights above 400 hPa, between 400-700 hPa and below 700 hPa respectively.

Ref. number	Feature name	AR	Status	AR10
Geostationary: low-level (below 700 hPa)				
2.3	GOES winter negative bias over NE America	2,3,6	Still present. Feature background: AR3 highlighted observations over land with a high height bias relative to the level of best-fit. This was linked to low level winds assigned to cloud base over sea, but not over land. AR6 showed a negative bias also observed over the N. Atlantic during cold air outbreaks which is linked to model forecast bias and difficulties in tracking the breakup of cloud along the SST front.	
2.6	MSG positive bias over N Africa	2,3,4 ,6	Still present. Feature background: A large positive wind speed bias is observed in the Meteosat Second Generation (MSG) IR and visible channels over North Africa and the Arabian Peninsula during winter. Although mainly over land, the bias extends over the Atlantic to the west of Africa in January/February and moves northwards into the Mediterranean by May. AR4 linked the bias to large height assignment errors when tracking cirrus clouds, leading to very fast winds being assigned around 500 hPa too low. The feature closely matches the location of the sub-tropical jet stream. AR9 investigated positive biases over the Arabian Peninsula in July 2018 and July 2019. Case for 27 July 2018: IR channel shows AMVs are easterlies whereas background is west or north-westerlies. Observed pressures are typically 700-800 hPa, best-fit is 100-200 hPa. Imagery shows tracking thin cirrus moving from east to west. Appears to be a classic example of large height assignment error. Also noted lots of dust in the imagery but AMVs (600-700 hPa) for this appear to match the model well.	
5.2	MSG negative bias during Somali jet	5,6,9	Still present. Feature background: SEVIRI AMVs from Meteosat-8/9 and Meteosat-11 show a large negative wind speed bias during July and August in the NW Indian Ocean, near the Gulf of Aden. This feature seems to vary in strength from year to year. This time period coincides with the strengthening of the Somali Low-Level Jet. Previous investigation has shown the bias is due to instances of height assignment error, with slow upper-level vectors incorrectly assigned within the fast, low-level wind regime, and the influence of an island (Socotra) causing semi-stationary wave cloud formations within the jet.	

6.2	FY-2 bias during NE winter monsoon	6	Still present Feature background: a marked negative speed bias in the northern hemisphere during the winter months from November to March. AR6 indicates that the negative-biased observations may have been assigned too high.	
8.1	MSG (IODC) positive speed difference in the tropics	8,9	Still present Feature background: Meteosat-8 low level winds show a positive speed O-B and high RMSVD over the southern tropics of the Indian Ocean. Model and radiosonde profiles provide evidence for a lack of shear in the AMVs which leads to a positive speed bias above 900 hPa height. Best-fit pressure indicates this could be due to AMVs being assigned too high. See AR9.	
9.2	Large vector differences near the Southwest African coast	9	Still present Meteosat-10 and Meteosat-8 low level IR winds show an area of large vector differences along the Atlantic coast of Southern Africa.	
Geostationary: mid-level (400-700 hPa)				
2.8	Positive bias in the tropics for MSG, FY-2, GK-2A	2,3,4,5,6,7	Still present Feature background: Previous reports have noted that mid-level AMVs tended to have a positive speed bias in the tropics and a negative speed bias in the extra-tropics. As new generations of satellites and derivation schemes have been introduced this has no longer been the case, e.g. for Himawari, and GOES. In general, there are far fewer AMVs extracted at mid-level and biases are thought to be largely the result of height assignment errors.	
2.9	Negative bias in the extra-tropics for MSG, FY-2	2,3,4,5,6,7		
Geostationary: high-level (above 400 hPa)				
2.10	Negative speed bias in extra-tropics for MSG, FY-2 and GK-2A	2,3,4,5,6	Still present Meteosat: Still prominent in IR, less in WV7.3 and less again in WV6.2 (difference between channels). Meteosat (IODC): Almost semi-permanent area of negative bias over Asia which appears to mark the position of the Himalayan Plateau. FY-2: Strong negative bias in IR. GK2-A: Strong negative bias.	

2.13	Positive speed bias in tropics for MSG and FY- 2	2,3,4,5,6,7	Still present Meteosat: Positive bias still present. FY-2G: Positive bias in IR, less so in WV.	
2.14	High troposphere positive bias	2,3,6	Still present in MSG . Feature background: A positive speed bias for MSG AMVs assigned heights high in the upper troposphere. The bias may be due to a 'high' height assignment bias. There is a seasonal dependence affecting the EUMETSAT data: a positive bias can be observed between October-April, the rest of the year is dominated by a negative speed bias.	
2.15	Differences between channels	2,3,5	Zonal plots suggest there is still a large difference between IR and WV channels for MSG. GOES and Himawari only show small differences.	
3.2	Negative Speed bias in Tropical Easterly Jet (TEJ) strongest over the Indian ocean.	3,6	The zonal plots for MSG IR for August 2022 show the bias is still worse versus the Met Office than versus ECMWF. Feature background: A negative speed bias for MSG winds in the high-troposphere of the tropics between June and September. Previously shown to be a contribution from the Met Office model error linked to an excessive TEJ in the analysis.	
4.2	GOES negative bias in tropical Pacific	4,5,6	Still present for GOES Feature background: GOES West exhibits a negative speed bias from December to April. Model errors are thought to contribute to the O-B signal which has also previously been shown to vary from year to year indicating some synoptic dependence.	
9.5	Negative speed bias in tropics for GOES	9	Still present Feature background: A negative bias in both IR and WV channels.	
Leo and mixed AMVs				
2.19	Aqua WV high-level positive speed bias	2,3,4,5	Still present for Aqua WV.	
2.20	Low-level negative speed bias	2,3,4	Still present in CIMSS AVHRR and NESDIS MODIS. Not apparent in Suomi NPP.	

4.3	Near-pole mid-level negative bias 4,5	4,5	More of a general negative bias for CIMSS and MODIS winds.	
7.1	Dual-Metop high level positive bias in tropics	7	Still present. Feature background: It has been noted that there are differences in the characteristics between the different Metop image pairs, in terms of time gap, overlap extent and viewing geometries. The geometry is important as the AVHRR pixel size varies from 1km at nadir to 4km at the edge of the swath.	
7.2	EUMETSAT Metop high level negative bias in midlatitudes	7	Still present. Feature background: A negative speed bias affecting single and dual Metop winds between 20-20 degrees latitude at upper levels.	
7.3	MISR positive bias over ice and desert	7	We are no longer monitoring MISR winds, so cannot comment if this continues to be a problem. Feature background: MISR often shows a positive speed bias and large mean vector difference at low level over ice and desert. The low heights are believed to be due to tracking cloud shadows rather than the clouds themselves. Since the shadows have no apparent north-south motion due to parallax as is seen for clouds, they are assigned heights very close to the surface.	
7.5	MISR bad orbits	7	We are no longer monitoring MISR winds, so cannot comment if this continues to be a problem. Feature background: Monitoring of MISR AMVs often reveals stripes of data with large O-B differences. These are usually over the Atlantic or Pacific oceans. MISR winds retrieval requires visible landmarks to calibrate its camera geometry. The near-real time MISR winds processing is done with 10-50 minute data sessions. A session's data quality can be degraded if the Terra satellite does not pass over enough land to calibrate its cameras during that session.	
7.6	VIIRS square distribution	7	Still present in Soumi NPP and NOAA-20. Coverage restricted by a hard limit used to define the box size for the polar projection during the derivation process	
9.4	EUMETSAT Metop low level AMVs in winter hemisphere	9	Still present Feature background: Metop low level winds have a speed bias and large vector difference in the winter hemisphere. Imagery suggests the AMVs could be erroneously tracking surface features.	
General issues				

9.1	Orographic effects	9	Meteosat have semi-permanent area of negative bias over Asia which appears to mark the position of the Himalayan Plateau. Apparent in all 3 channels and all year, apart from JJA. Not seen in Himawari (just about has coverage), INSAT or in dual Metop. There is a consistent 50 hPa height difference between Meteosat-8 and other AMVs in this area. This height bias has less of an impact in summer when the vertical wind shear is less.	
9.3	Differences between Met Office and ECMWF statistics for Himawari	9	ECMWF has smaller mean vector differences at upper levels, Met Office has smaller mean vector differences at mid-level in tropics. There are differences also in biases at mid-level. There are differences in the use of Himawari data in data assimilation between the centres, but biases probably reflect wider NWP model difficulties in this area.	
10.1	Problems in regions of organized convection in the tropics.	10	In the tropics there are periods when there are strongly organized convective clusters. These clusters sometime become large and develop their own mesoscale system and many AMVs are produced from their high-level clouds. Sometimes forecast models fail to capture these systems and leads to large O-B departures.	Y

Table 3. Status of the active features identified in the AMV monitoring. Green shading denotes a new feature. Blue denotes a feature than is fixed or considered closed. The AR column lists the analysis report numbers where the feature is discussed.

3. Assessment of new data

There have been four recent geostationary satellite swaps. The first three are considered here. We have included a brief summary of the data quality from the new satellites compared to those they replaced. Other monitoring plots are available from the Monthly NWP SAF Monitoring site,

https://nwp-saf.eumetsat.int/site/monitoring/winds-quality-evaluation/amv/amv-monthly-monitoring/.

Meteosat-9 IODC

EUMETSAT replaced Meteosat-8 with Meteosat-9 as the Indian Ocean Data Coverage (IODC) service on 31 May 2022. A parallel period of Meteosat-9 was provided from 9 May - 31 May and this was monitored alongside the same data from Meteosat-8. The monitoring confirmed the O-B statistics were very close and the data were suitable for operations.

Examples of Meteosat-8/9 2D histograms of O-B above 400 hPa and vertical mean cross sections are shown in Figure 1 and Figure 2.

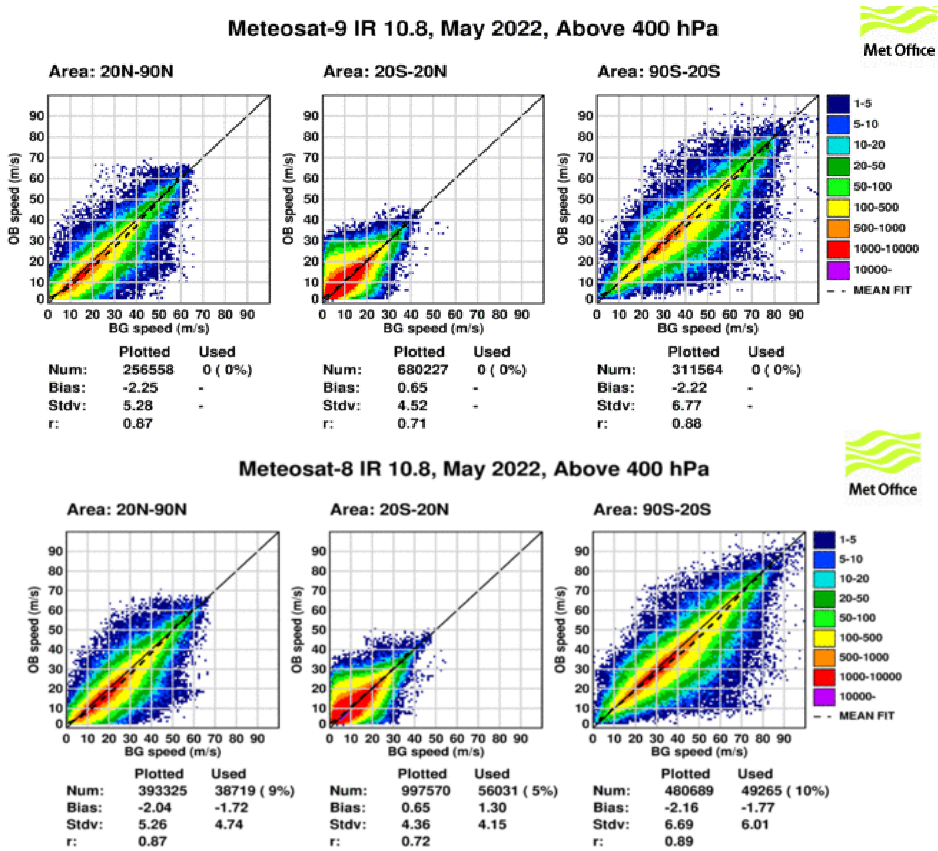

Figure 1. Meteosat-8/9 May 2022 monthly NWP SAF monitoring of O-B 2D histograms above 400 hPa.

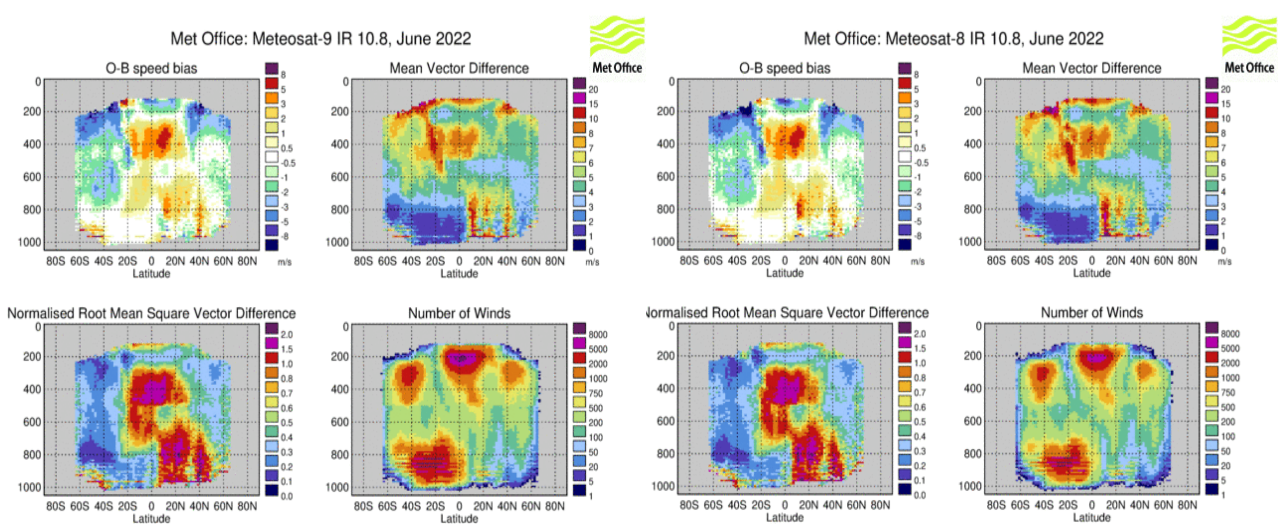

Figure 2. Meteosat-8/9 May 2022 monthly NWP SAF monitoring of vertical mean cross sections.

GOES-18

GOES-18 parallel data were monitored alongside GOES-17 and a short evaluation was performed. The GOES-18 data were shown to be consistent with GOES-17 but with the advantage that they are not impacted by the ABI instrument cooling issues suffered by GOES-17. This resulted in some improved statistics for GOES-18 during the GOES 17 ABI warm periods and a small increase in data volume. An example of 2D histograms above 400 hPa and vertical mean cross sections are shown in Figure 3 and Figure 4. Figure 4 shows reduced mean vector differences for GOES-18 at mid-level in the tropics and also a small increase in data volume.

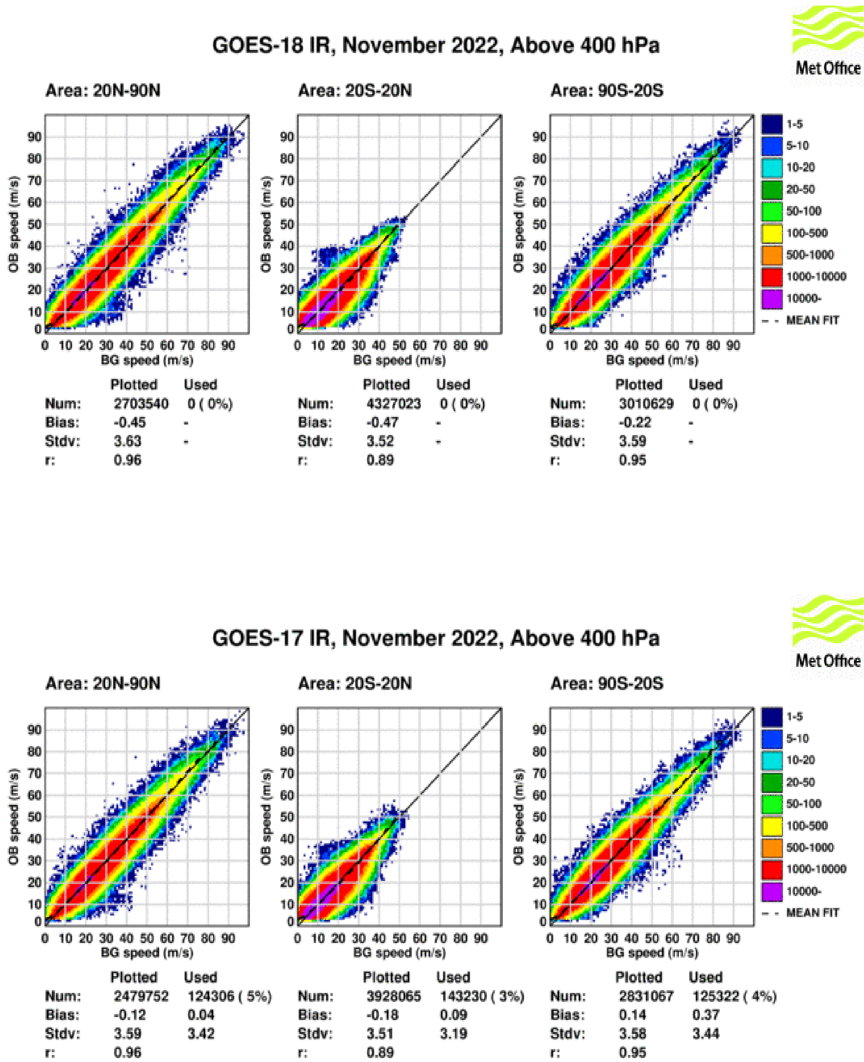

Figure 3. GOES-17/18 November 2022 monthly NWP SAF monitoring of O-B 2D histograms above 400 hPa.

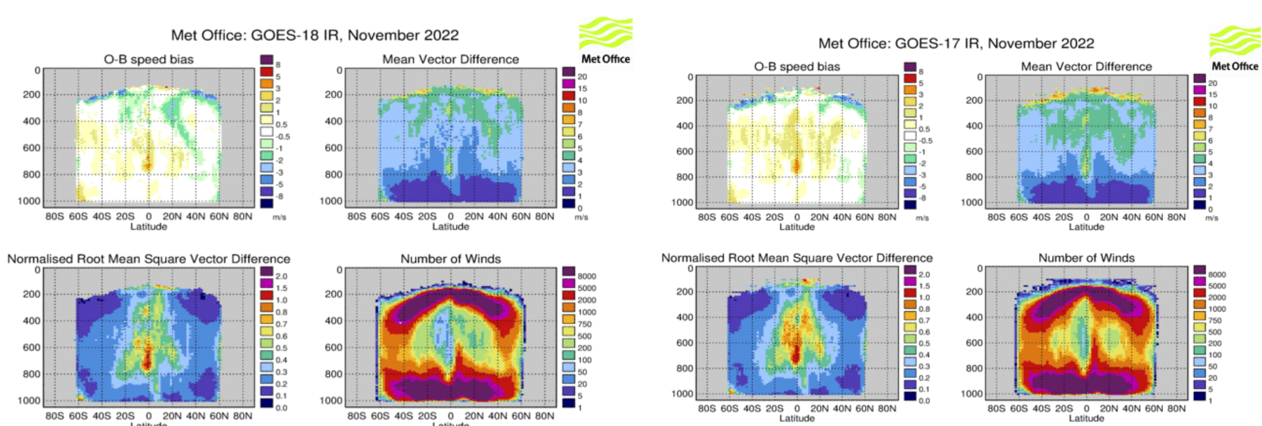

Figure 4. GOES-17/18 November 2022 monthly NWP SAF vertical mean cross sections.

Himawari-9

A parallel period of Himwari-9 test data were made available by JMA from 27 Sept - 6 Dec 2022. Very little difference could be seen between the satellites in the monitoring, and this was confirmed by collocation plots provided by JMA and from other NWP centres. An example of 2D histograms above 400 hPa and vertical mean cross sections are shown in Figure 5 and Figure 6.

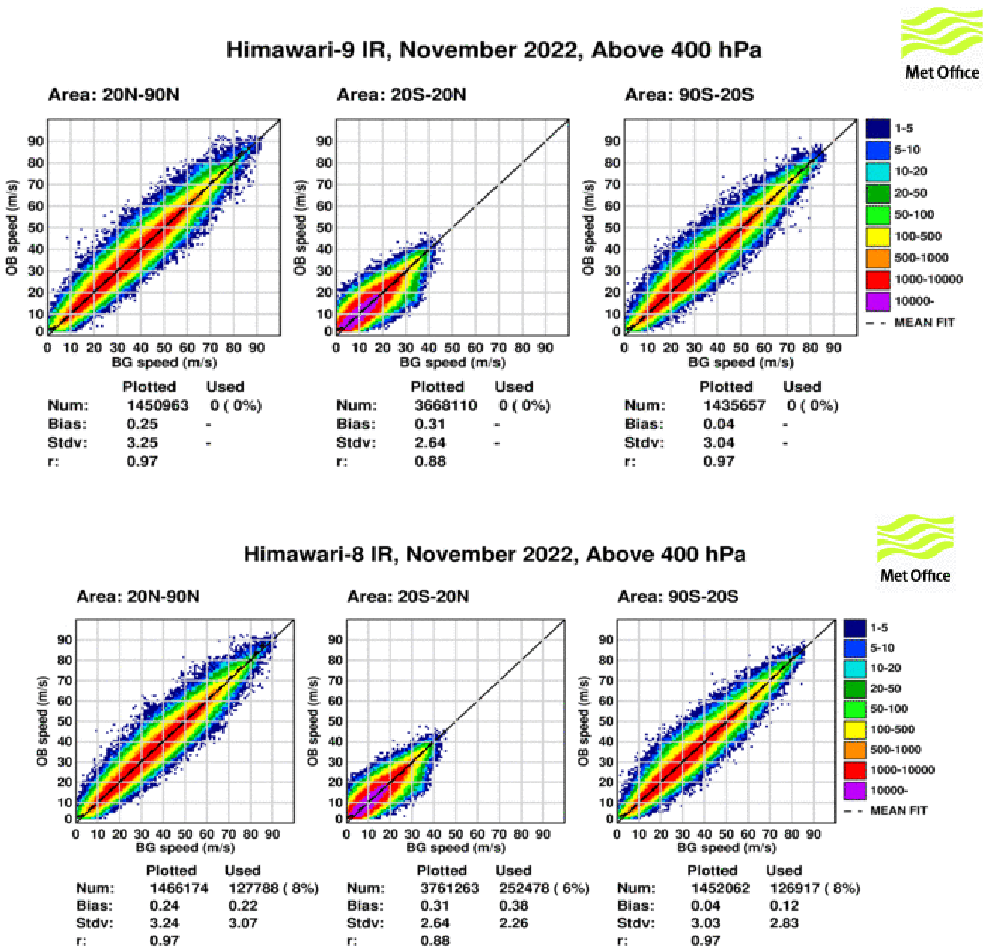

Figure 5. Himawari-8/9 November monthly NWP SAF monitoring of O-B 2D histograms above 400 hPa.

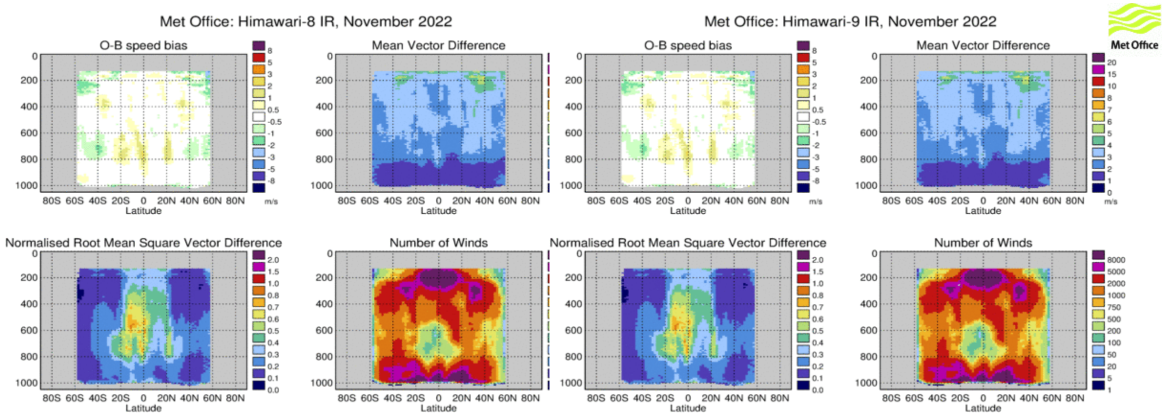

Figure 6. Himawari-8/9 November monthly NWP SAF monitoring vertical mean cross sections.

4. General thoughts on plot comparisons

Comparing plots from different geostationary satellites

Some examples of the O-B monthly NWP SAF monitoring for Meteosat-11, GOES-18 and Himawari-9 are compared in Figure 7. Generally, O-B plots for Meteosat-11 show larger differences than both GOES-18 and Himawari-9. This increase in O-B statistics may not reflect poorer quality of the Meteosat-11 AMVs but be more related to how the model NWP information is used during the AMV derivation procedure.

The NWC SAF winds intercomparison study (Santek 2023, pp 207) found similar results. In this study there was a useful questionnaire response from the AMV producers about the use of temporal filtering and NWP model information in their processing. The intercomparison report also suggests the larger Meteosat AMV errors may be due to the lighter use of NWP background information.

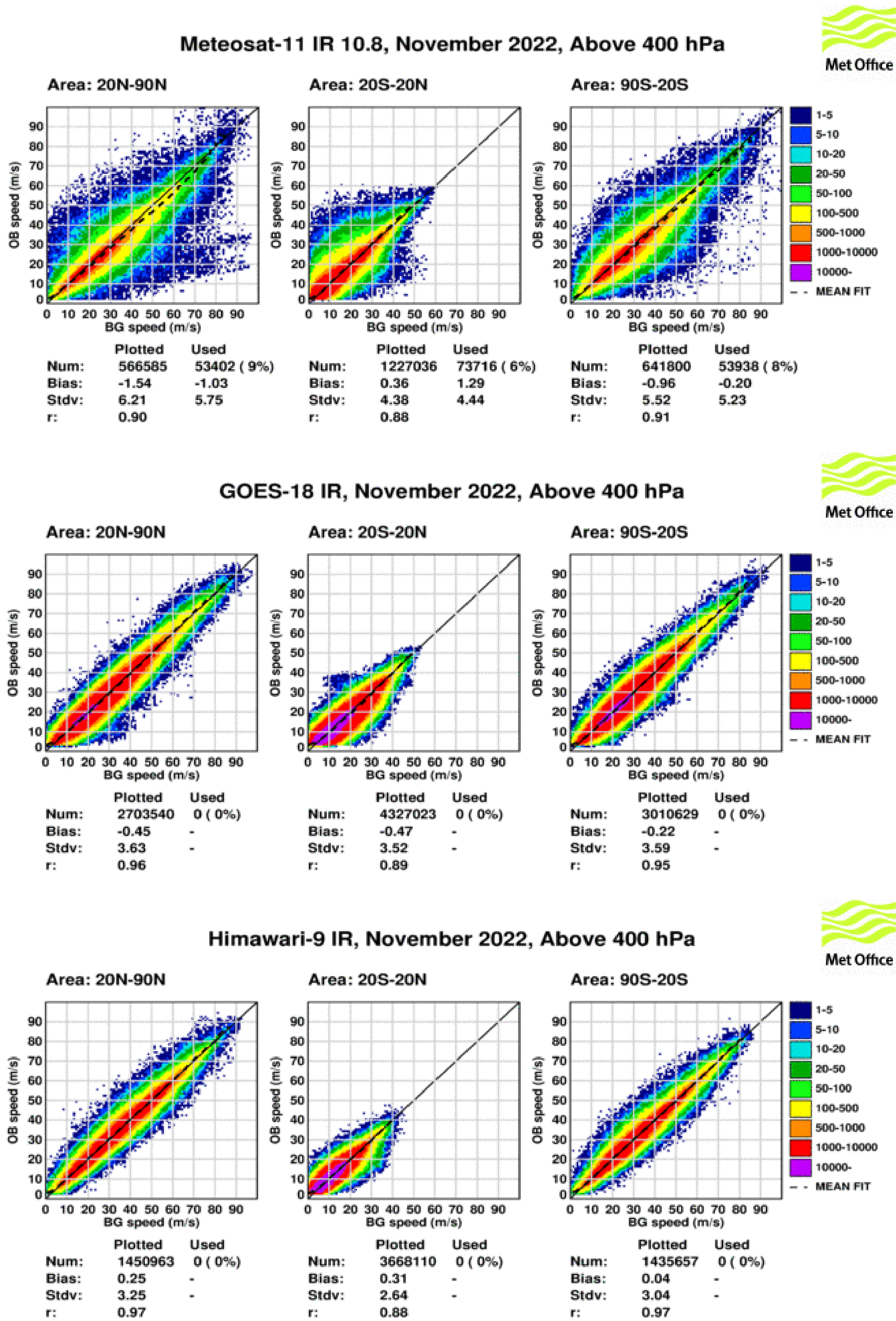

Figure 7. Meteosat-11, GOES-18 and Himawari-9 IR monthly NWP SAF monitoring of O-B 2D histograms above 400 hPa for November 2022.

Comparison of Meteosat-11 O-B statistics between ECMWF and the Met Office

AMV O-B departures are calculated against the Met Office and ECMWF global models to give insight into whether features seen in the monitoring are related to any difference between the models. These O-Bs from the AMVs are used as a common reference. Some pairs of the monthly NWP SAF monitoring plots for Meteosat-11 for ECMWF and the Met Office are shown in Figures 8 and 9.

The O-B 2D histograms statistics plots in Figure 8 show that the number of observations between centres are very close, there is a very small difference in the standard deviation, for example ECMWF, NH, 6.1 m/s, Tropics, 4.1 m/s, SH, 5.2 m/s, compared to the Met Office NH, 6.2 m/s, Tropics, 4.4 m/s, SH, 5.2 m/s. These small differences could be partly due to the use of ECMWF forecasts in the EUMETSAT AMV processing.

A dual comparison of the O-B statistics vertical mean cross sections, in Figure 9, suggests that the 6-hour forecast of ECMWF and the Met Office are very similar.

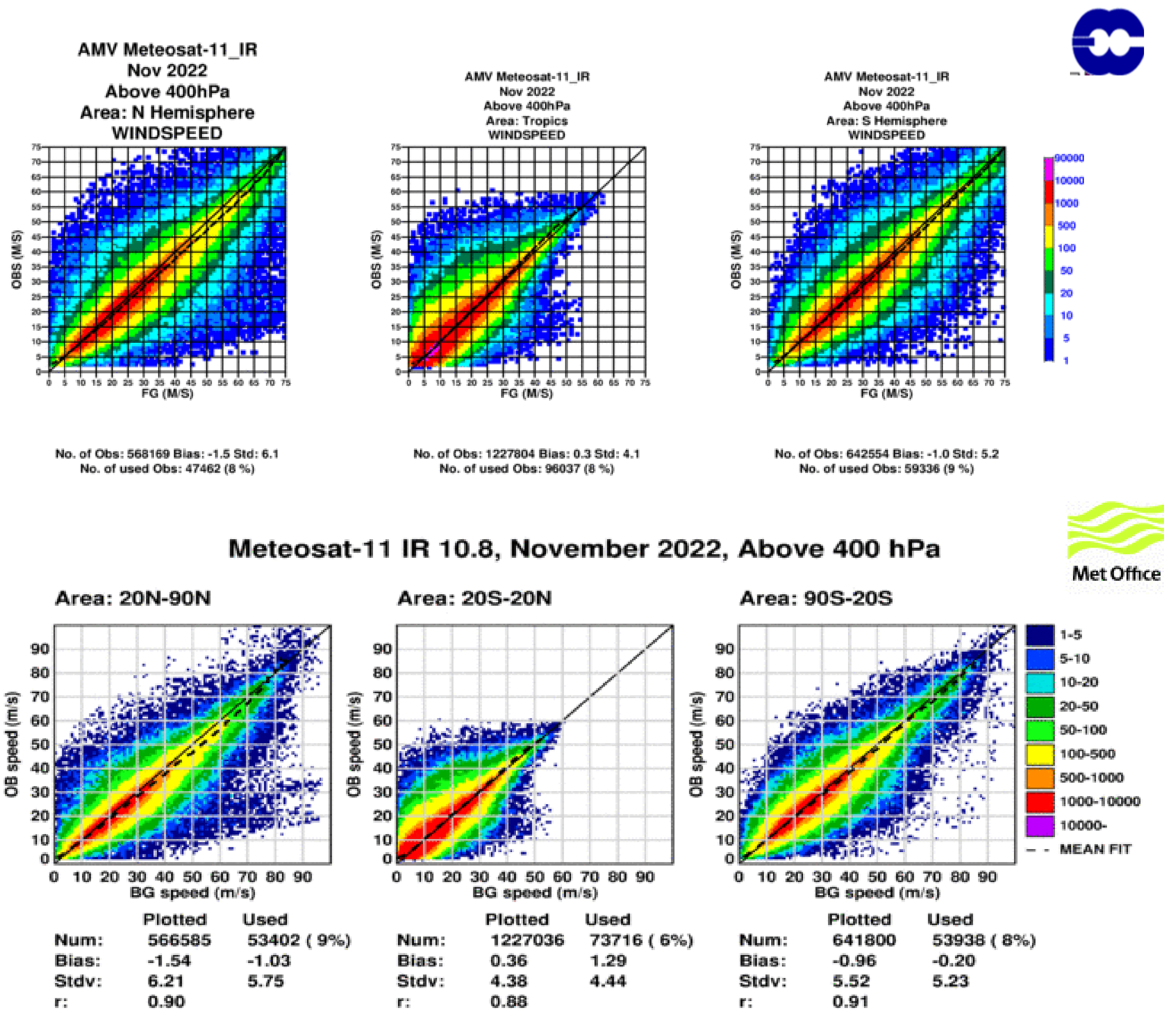

Figure 8. ECMWF and Met Office density plots for Meteosat-11 IR high level, November 2022.

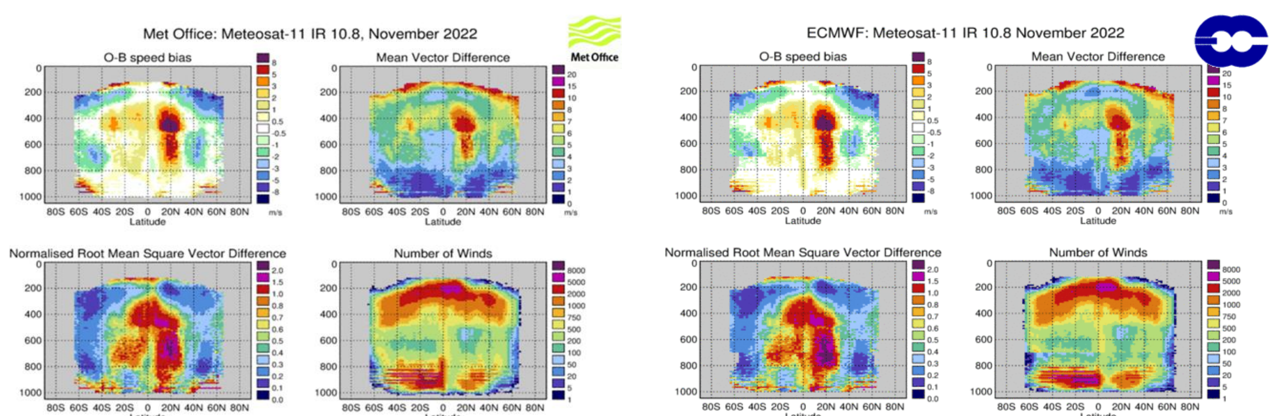

Figure 9. ECMWF and Met Office cross sections for Meteosat-11 IR, November 2022.

Comparison of Meteosat-11 AMV statistics between EUMETSAT and NWC SAF packages

EUMETSAT sponsors a Nowcasting Satellite Applications Facility (NWC SAF) that has developed several nowcasting software products (including calculating AMVs) based on Meteosat, GOES and Himawari satellite imagery. The software is accessible through the NWC SAF website http://www.nwcsaf.org/

At the Met Office, the NWC SAF software is routinely run over the UK region (Milan et al.2020) to provide timely and high resolution AMVs for the Met Office UKV mesoscale data assimilation. Routine AMV monthly monitoring (O-B) can be found on the NWP SAF AMV monitoring web site.

In this UK region O-Bs are calculated for the UK NWC SAF and EUMETSAT AMVs, and are compared in Figure 10 for November 2022. These two AMV processing methods have many similarities (Santek 2023). However, there are some differences: the local UK NWC SAF package provides the data assimilation AMVs every 15 minutes compared to hourly for EUMETSAT (EUMETSAT produces 15 minute AMVs but only sends on the Global Telecommunication System hourly data). The SAF package chooses up to three tracers for each segment compared to one for the EUMETSAT AMV package.

Two things to note in the comparison in Figure 10 are the difference in data volume and a general improvement in overall statistics. Similar improvements between the UK NWC SAF and EUMETSAT AMV packages have also been reported in the intercomparison report (Santek 2023).

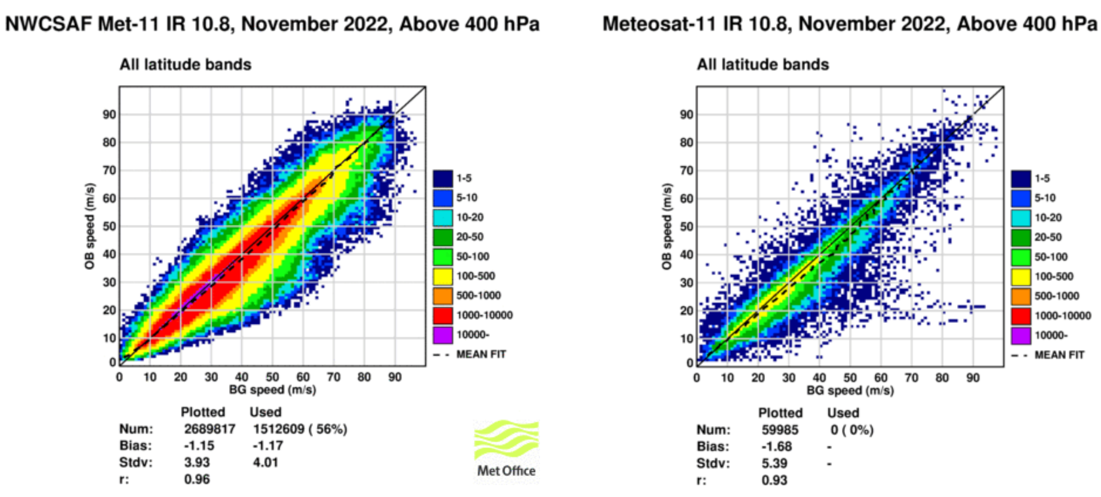

Figure 10. Current NWC SAF Meteosat-11 and EUMETSAT Meteosat-11 November 2022 O-B monthly monitoring for the UK area.

5. Use of the NWC SAF package in the Tropics

The NWC SAF processing package was configured over the Tropical Eastern African region (3S 25N, 30W 20E) to investigate the value of high density AMVs to understand tropical convective systems. Extra diagnostic information was also retained during the AMV processing, which is not available from AMV providers, in particular AMV cross-correlation matrices.

A brief summary of the NWC SAF processing package follows. For a full description of the NWC SAF AMV processing chain refer to:

https://www.nwcsaf.org/Downloads/GEO/2021/Documents/Scientific_Docs/NWC-CDOP3-GEO-AEMET-SCI-ATBD-Wind_v1.0.1.pdf

1. *Pre-processing:*

   • This includes reading and geolocation of the satellite data, reading of the NWP model data and using earlier processed cloud products from the NWC SAF package.

2. *Processing:*

   • Tracers are calculated.

   • These tracers are tracked using the next satellite image using cross-correlation. If none of the elements in this cross-correlation matrix has reached 0.8 then the tracer is rejected.

   • AMVs are then calculated using their tracer displacements and other cloud parameters from the earlier pre-processing.

3. *post-processing*:

   • A series of quality control steps are performed and a quality indicator (QI) value is assigned for each AMV.

Use of cross-correlation matrices

A modified version of the NWC SAF package was run over the UKV region with the UKV model for two months. The output O-B data set included cross-correlation matrices. It was found that features of the cross-correlation matrix, such as the strength and uniqueness of central maxima were related to AMV O-Bs (Kelly, 2021).

This study demonstrated that the structure of the cross-correlation matrices is a useful method to identify poor AMV tracers.

Examples of strong cross-correlation matrices.

An interesting case is shown in Figure 11, where there is a group of AMVs which differs in wind direction from the neighbouring AMV fields by 180 degrees. This is shown in the red box and an expanded view is shown in Figure 12.

Two examples of AMV cross-correlation surfaces for the two wind flows are shown in Figure 12. Both cross-correlation surfaces are typical cross-correction surfaces of their near neighbours. These surfaces are examples of well-constrained cross-correlation surfaces indicating good tracking. The AMV from the upper cross-correlation plot is from a southeast direction at 300 hPa. The AMV from the lower cross-correlation plot is from a northwest direction at 196 hPa. The AMVs suggest the underlying clouds are moving in the opposite direction to the upper clouds. There is also good agreement between the AMVs and their model guesses, (AMVs (yellow) and model guess (blue)).

Initially, it was thought that there may be a problem with the AMVs, however the good cross-correlation surfaces and agreement with the model suggests the AMVs are correct, but that there is strong vertical wind shear in this region.

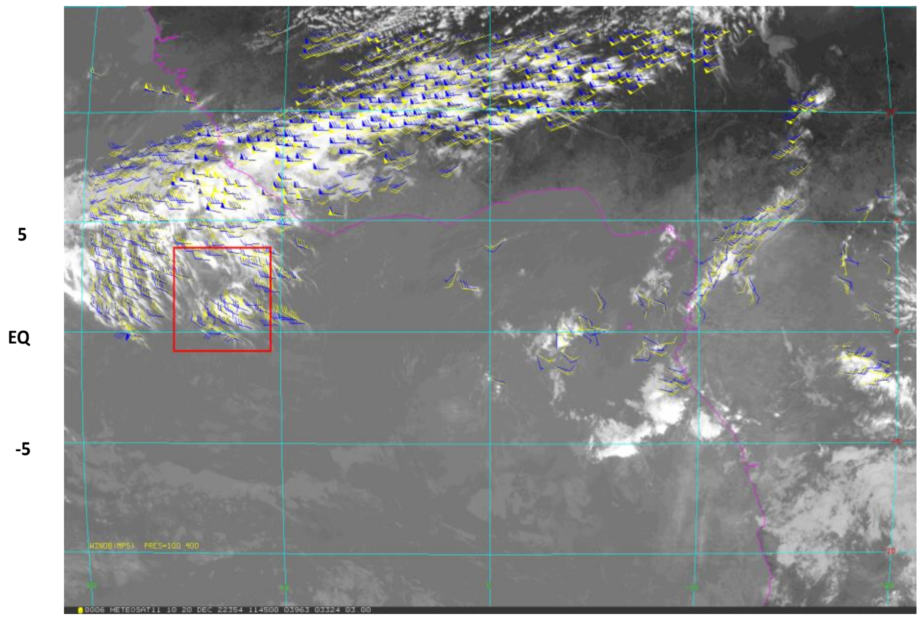

Figure 11. 11:45 UTC on 20/12/2022. Comparison of NWC SAF AMVs (yellow) and model guess (blue) in an upper-level cloud band.

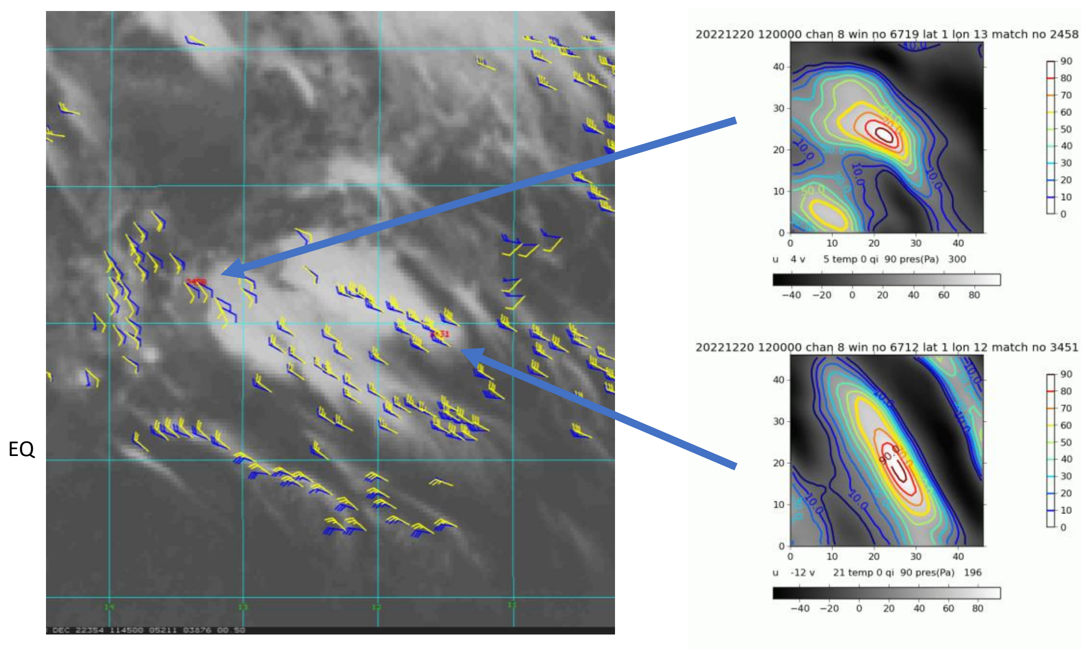

Figure 12. 11:45 UTC on 20/12/2022. Expanded view of the red box in Figure 11. Underlying clouds (300 hPa) are moving in the opposite direction to the upper flow (196 hPa) NWC SAF AMVs (yellow) and model guess (blue).

6. Validity of AMVs in the African Tropical region

The African Tropical region in August is usually a very stormy time in comparison to March. The upper-level mean O-B plots from Meteosat-11 (Figures 13,14) shows slightly larger tropical biases in August and the O-B density plots (Figure 15) are very different. The O-B Standard Deviation (Stdv) in March is 3.8 m/s compared with the much larger value of 5.4 m/s for August.

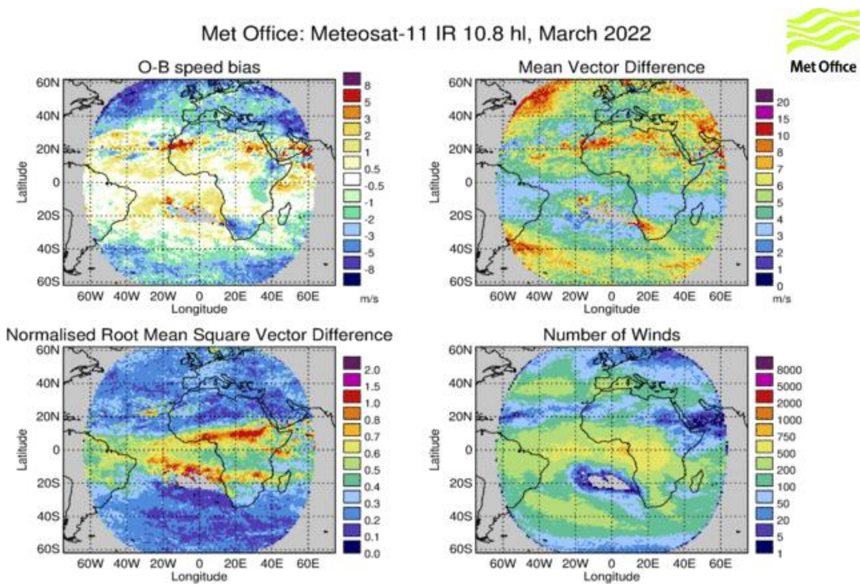

Figure 13. Monthly monitoring map plot for Meteosat-11 IR high level for March 2022.

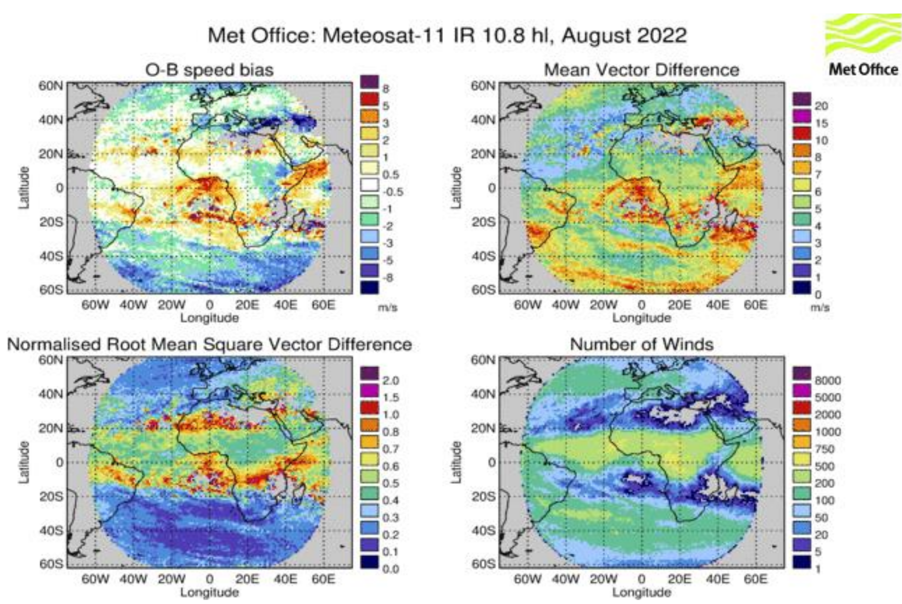

Figure 14. Monthly monitoring map plot for Meteosat-11 IR high level for August 2022.

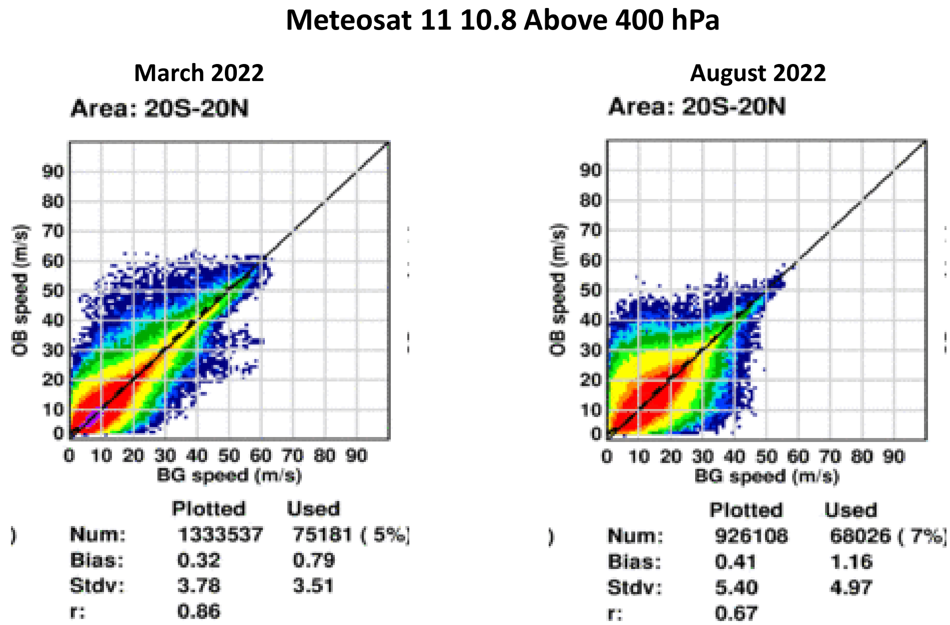

Figure 15. Density monthly monitoring plot for Meteosat-11 IR high level for March and August 2022.

6.1 Differences in an MCS over Western Africa

In this region, during August, the cloud clusters grow very large and often become well organized into large mesoscale convective systems (MCSs). These systems usually drift eastward from central Africa into the tropical Atlantic and on some occasions become tropical cyclones.

Figure 16 shows the Meteosat-11 image for 1145 UTC on 24 August 2022. The EUMETSAT GTS AMVs between 100-400 hPa are shown in red and their NWP guess in blue. The AMVs plotted have QI (using forecast guess) greater than 0.7. At first sight, there appears to be reasonable agreement between the AMVs and model guess in wind direction. However, in the next figures the image area will be reduced several times to reveal more detail and the QI test will finally be removed.

The region chosen to study is centred at 10 degrees North and 15 degrees West which includes two major MCSs. During August the NWC SAF package, as described in Section 5, was running routinely over this region. Figure 17 shows a comparison between high level EUMETSAT AMVs (red) and NWC SAF AMVs (blue) using the QI with values greater than 0.7.

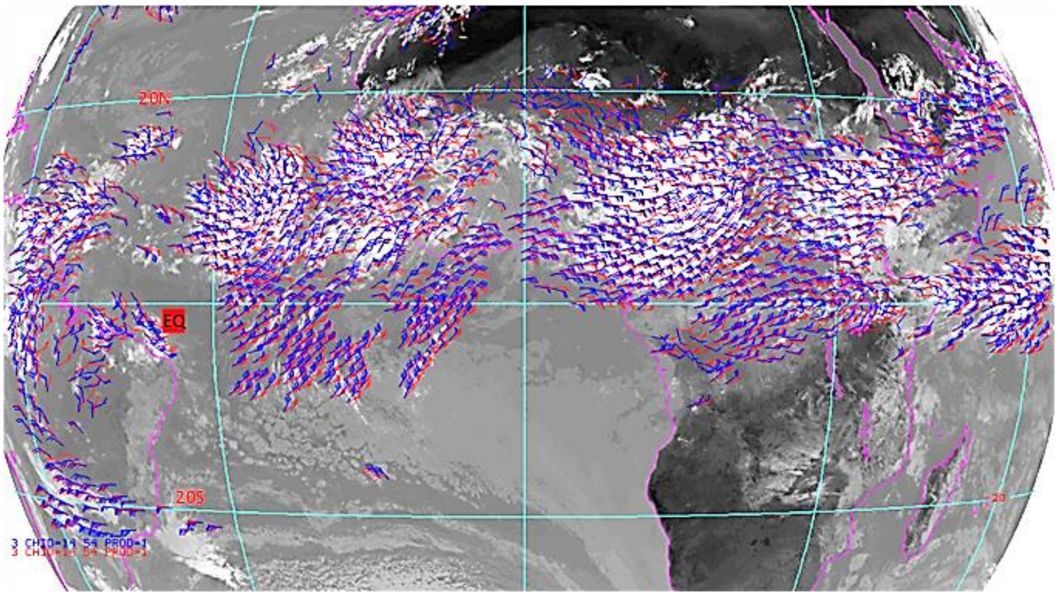

Figure 16. 11:45 UTC on 24/08/2022. *AMVs between 100-400 hPa: EUMETSAT AMVs (red), NWP guess (blue).*

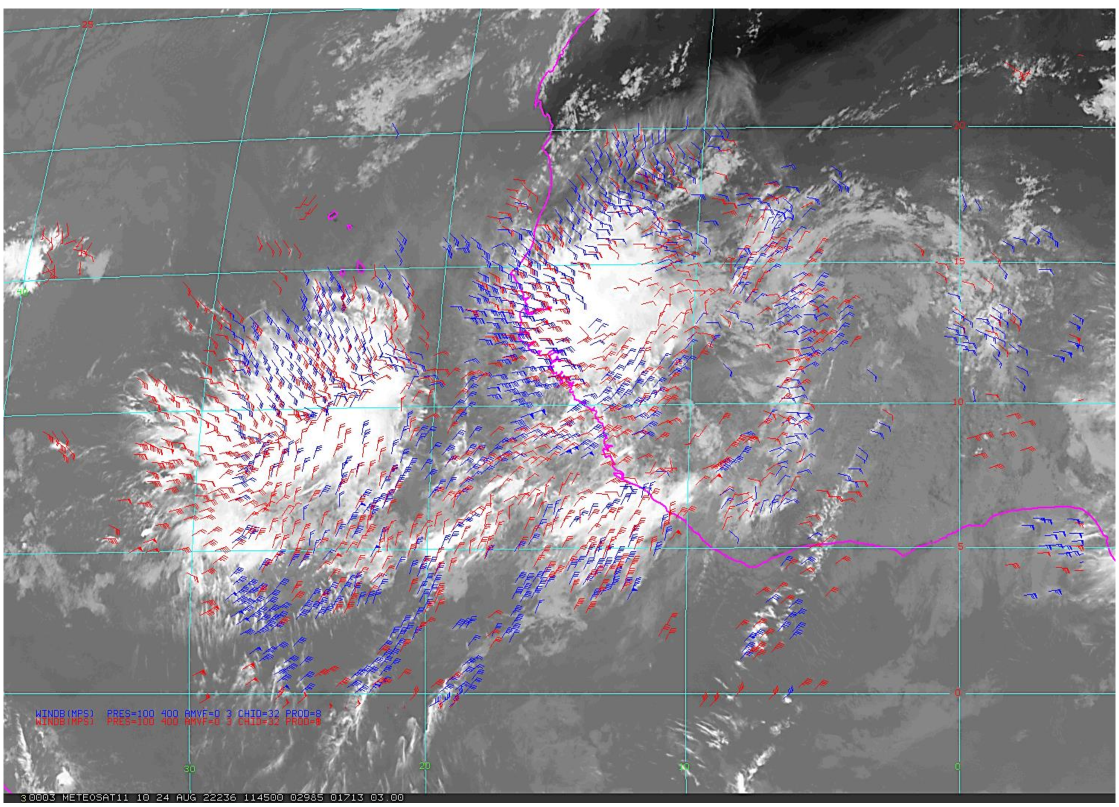

Figure 17. 11:45 UTC on 24/08/2022. AMVs with QI values greater than 0.7 between 100-400 hPa: EUMETSAT AMVs (red), NWC SAF AMVs (blue).

Both sets of AMVs agree closely in direction, but the coverage varies due to differences in parameter settings for each AMV processing package. Note the NWC SAF processing boundary is about 20-degrees west. In some regions the different coverage may be caused by differences in QI value between the packages. With reference to Figure 10 there is an increase in data volume for the NWC-SAF AMVs compared with the EUMETSAT package.

Figure 18 shows NWC SAF AMVs in red and NWP guess in blue with no QI check applied. Now it is clearer to see there are many AMVs that differ in direction from their model guess.

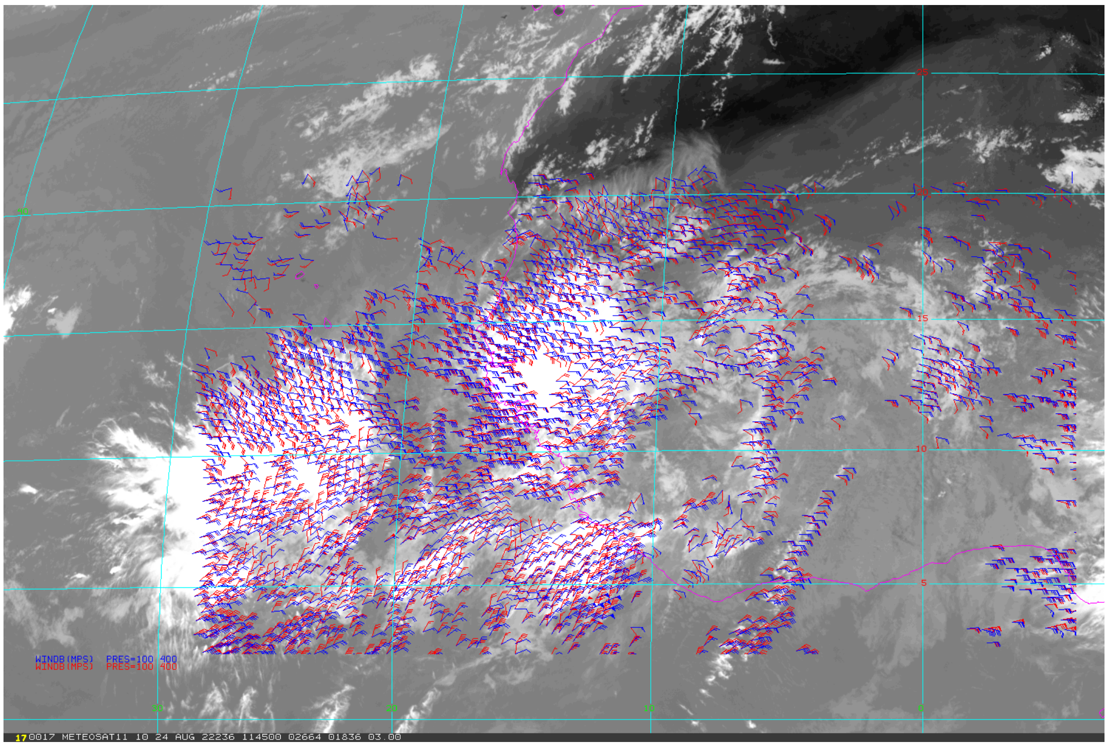

Figure 18. 11:45 UTC on 24/08/2022. All AMVs between 100-400 hPa: NWC SAF AMVs (red), NWP guess (blue).

To investigate if there are any valid structures within these unfiltered AMVs, a region covering a large MCS over Africa in the center of Figure 18 was chosen, see Figure 19 and the attached movie :

https://nwpsaf.eu/monitoring/amv/animations/m11ir108_20220824.gif

The movie is five frames every 15 minutes from 11:00 UTC and shows the cloud motion (high clouds white). Superimposed on all images are the NWC SAF all AMVs (red) and the model guesses (blue) at 11:45 UTC. The motivation for freezing the NWC SAF AMV observation time is to observe if the clouds do not greatly change their identity between frames during the tracking.

There are few NWC SAF AMVs in the central region of the MCS, possibly due to the smooth cloud structure. However, towards the edge, the cloud becomes broken and many NWC SAF AMVs appear, particularly on the left side. Largely, the NWC SAF AMVs and model guess are consistent within themselves. However, the agreement in direction between the NWC SAF AMVs (red vectors) and model guess (blue vectors) is very mixed. On the left side of the MCS the directional differences are small but towards the lower right and center top, these differences in direction are often greater than 45 degrees. To compare the differences, each set of vectors were analyzed on a 0.3x0.3 deg grid using McIdas software (Hibbard,1990). Streamlines from each are shown in Figure 20 (magenta NWC SAF AMVs, blue model guess) the AMVs are clearly following the cloud motion as seen in the movie. The model does not contain any divergent flow ahead of the MCS and has not captured the MSC upper-level wind structure.

A further enlarged region, Figure 21, was chosen to look more closely at the NWC SAF AMVs and their forecast guesses. Earlier work (Kelly, 2020) has shown good tracer tracking relies on the structure of these cross-correlation matrices having a strong single isolated maximum. A typical example is shown in the top right of Figure 21. All cross-correlation matrices were examined in the Figure 21 region, and it was found that over 80% were rated as good for tracking. The other 20% of these cross-correlation matrices failed to have a single strong maximum. An example of a poor cross-correlation matrix is shown on the bottom right of Figure 21. There was no consistent pattern as to the location of these AMVs.

The upper-level flow, as captured by the AMVs, (Figure 20), shows the strongly divergent wind pattern ahead of the MCS, as would be expected. Unfortunately, the NWP model failed to capture this feature.

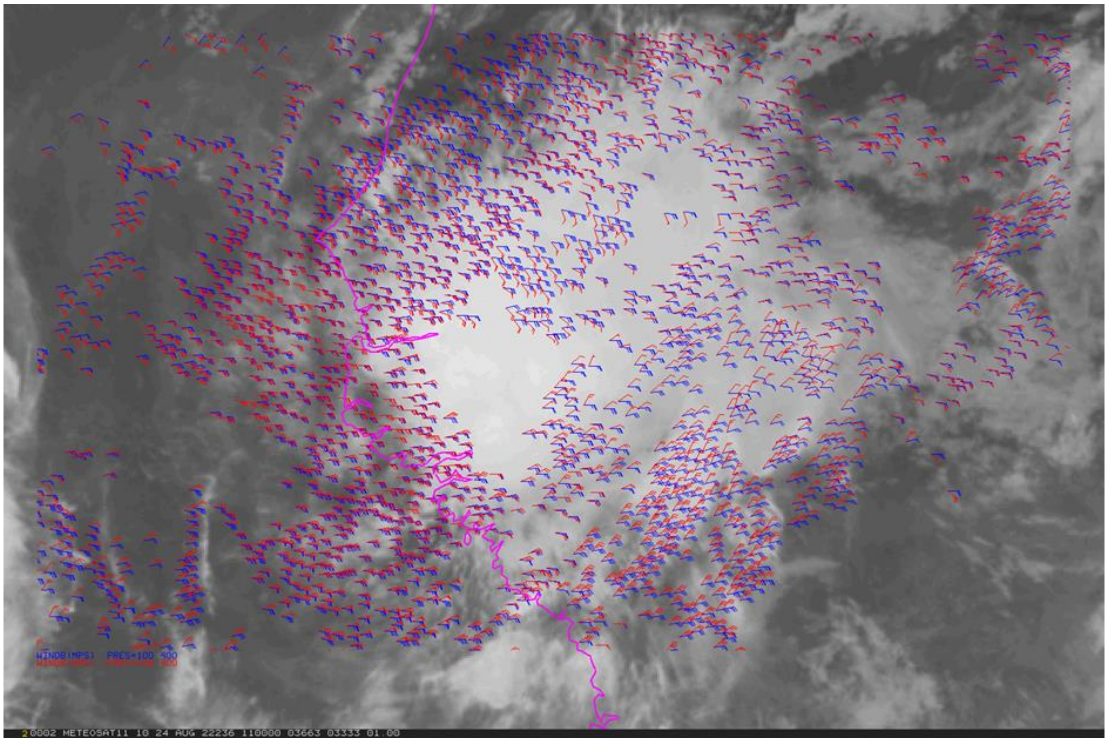

Figure 19. 11:45 UTC on 24/08/2022 The MCS from the same image as Figures 15,16 and 17. Red vectors are NWC SAF all AMVs and blue vectors model guess.

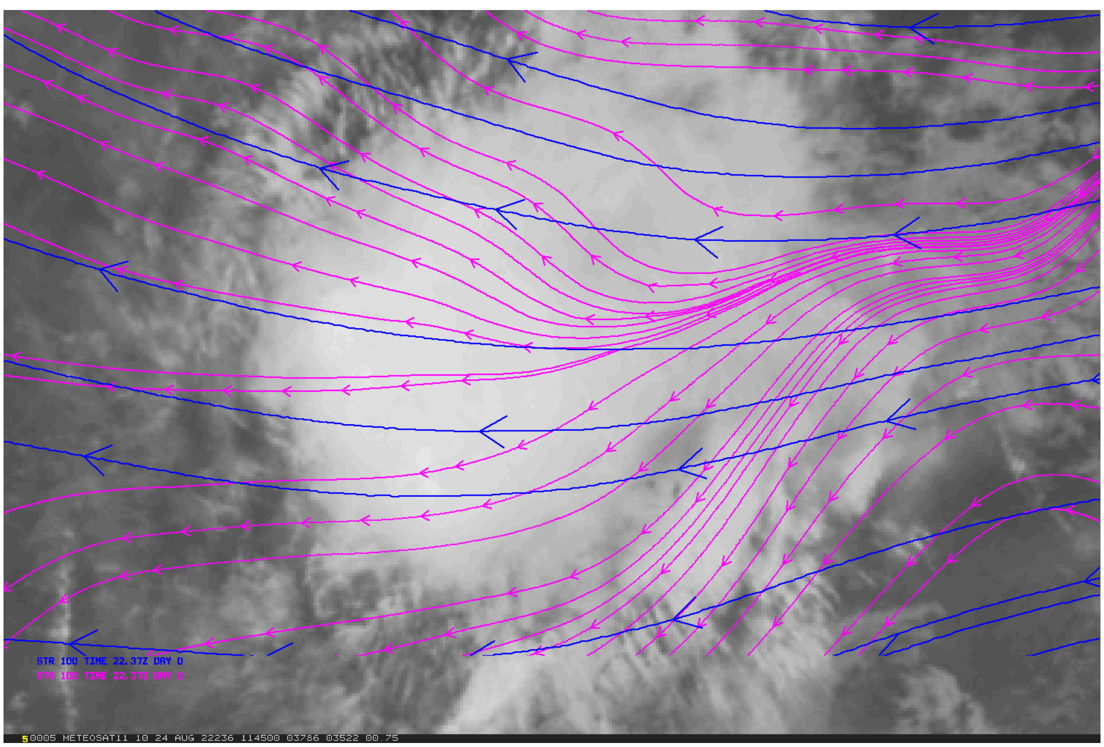

Figure 20. 11:45 UTC on 24/08/2022. The MCS from the same image as Figures 15,16 and17. Red vectors are NWC SAF AMVs and blue vectors model guess.

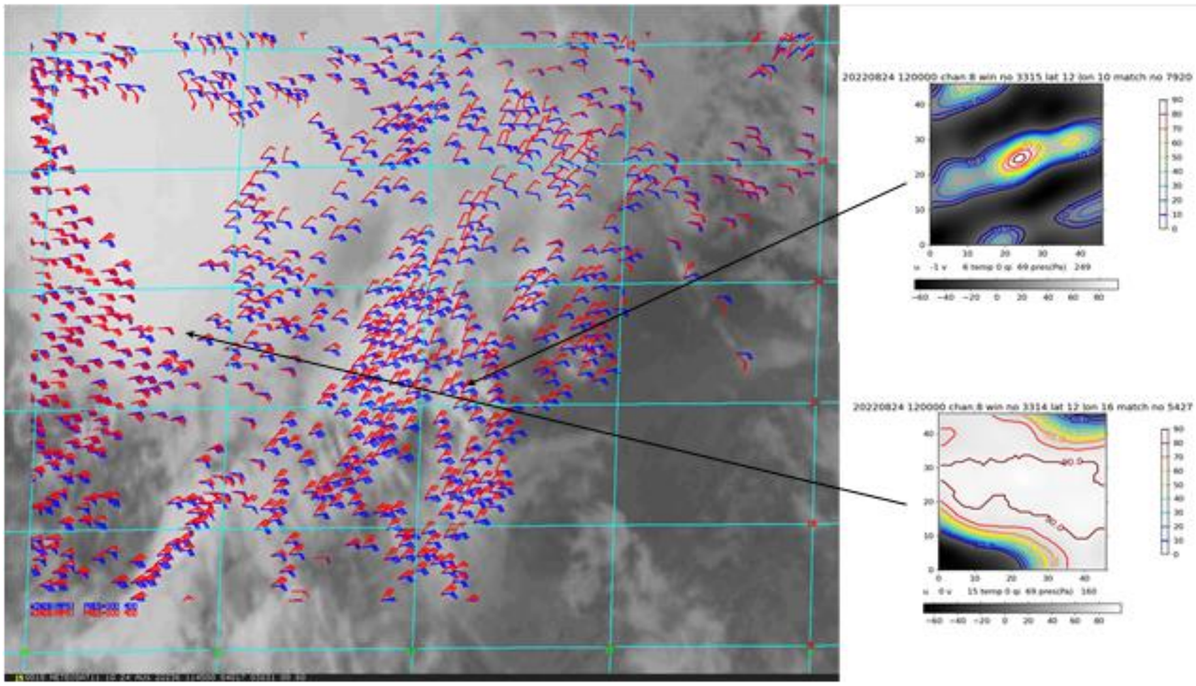

Figure 21. 11:45 UTC on 24/08/2022 Expanded view of Figure 18 including two cross-correlation matrices. Red vectors are AMVs and blue vectors are the model guess.

6.2. AMVs in the Tropical boundary layer assigned incorrect pressures

Figure 22 shows AMVs (blue) and model guess (yellow), together with scatterometer surface wind vectors (red). There is a systematic difference in wind direction between the NWC SAF AMVs and the model guesses. It is interesting that the scatterometer surface wind vectors are closer to the NWC SAF AMVs, suggesting the AMVs are derived from clouds moving in the same general direction as the surface flow.

Two cross-correlation matrices from AMVs in this region are shown on the right (Figure 22). These are typical of the low level AMVs in this region and have small and well-defined maxima suggesting that the cloud tracking is well constrained.

Figure 23 is a single frame of a five-frame movie of Meteosat-11 channel 2 from 11:30 to 12:30 UTC on 20/12/2022 and can be found at:

https://nwpsaf.eu/monitoring/amv/animations/m11ir108_20221220.gif

The movie shows low-level clouds in the left of the image over the ocean moving north. The northward motion of these clouds agrees with the direction of the NWC SAF AMVs (Figure 22).

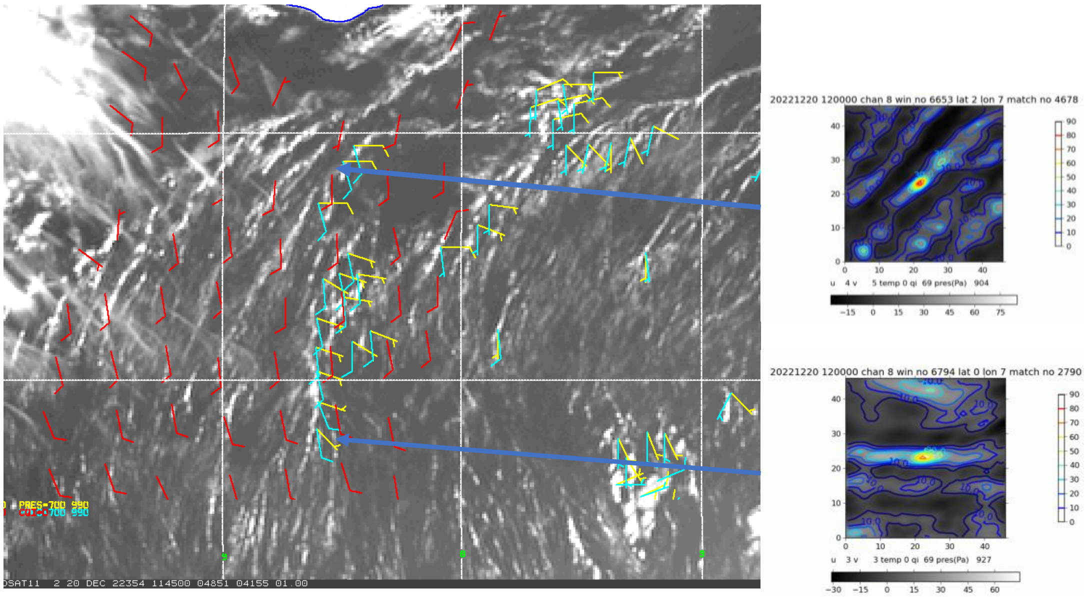

Figure 22. 11:45 UTC on 20/12/2022 Low level AMVs (blue), their model guess field (yellow) and scatterometer winds (red).

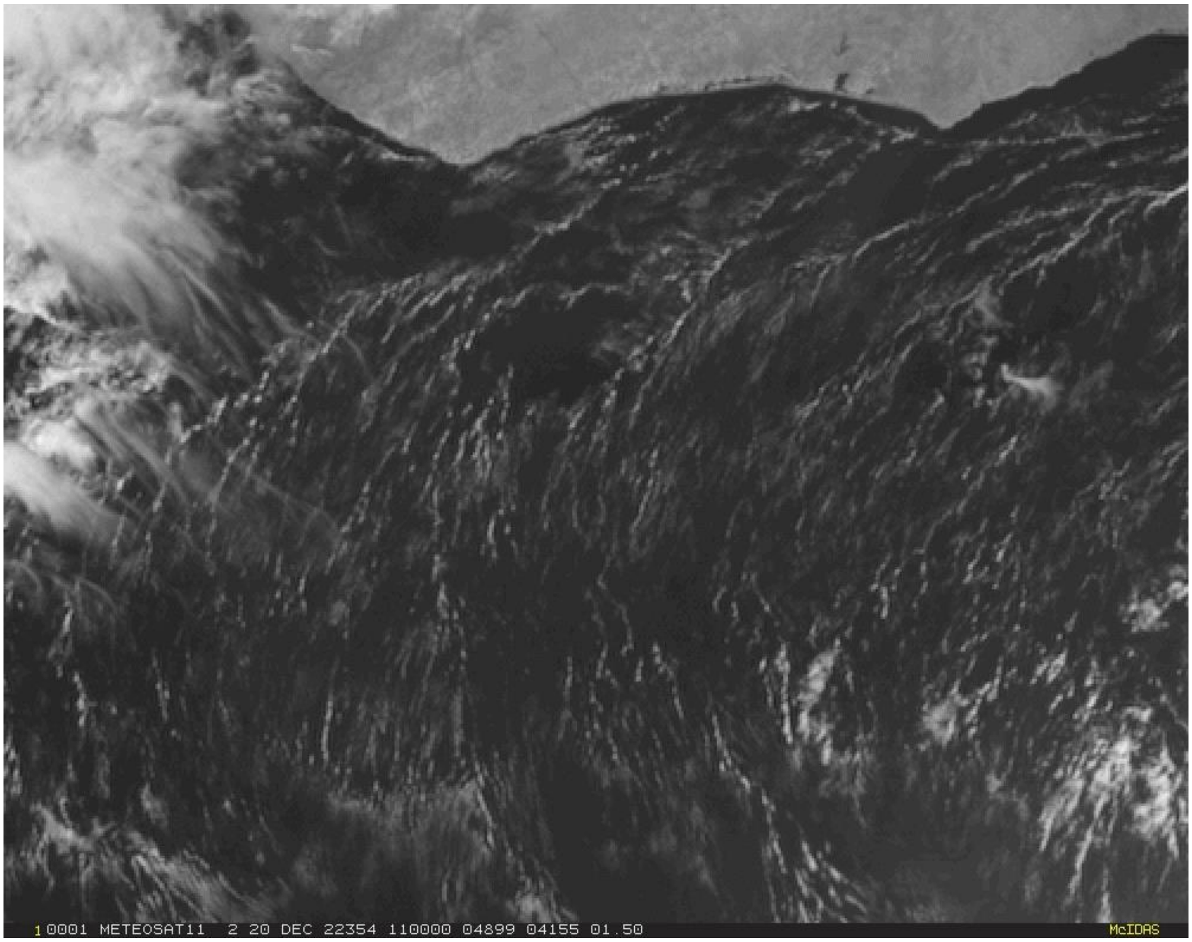

Figure 23. 20/12/2022 seven frames of 15-minute Meteosat-11 channel 2 from 11:00 to 12:45 UTC.

A model guess vertical profile of wind and humidity is shown in Figure 24, which was chosen from the AMV at the top left of Figure 22. At the bottom of this profile there is a sharp change in humidity and wind direction suggesting the top of the boundary layer. The reported AMV height is 904 hPa and above the top of the boundary layer. The model best-fit pressure estimate is poorly constrained in this case so should be ignored. Vertical profiles for other AMVs in this region also show the AMV reported heights to be above the boundary layer and show large direction differences from their guesses.

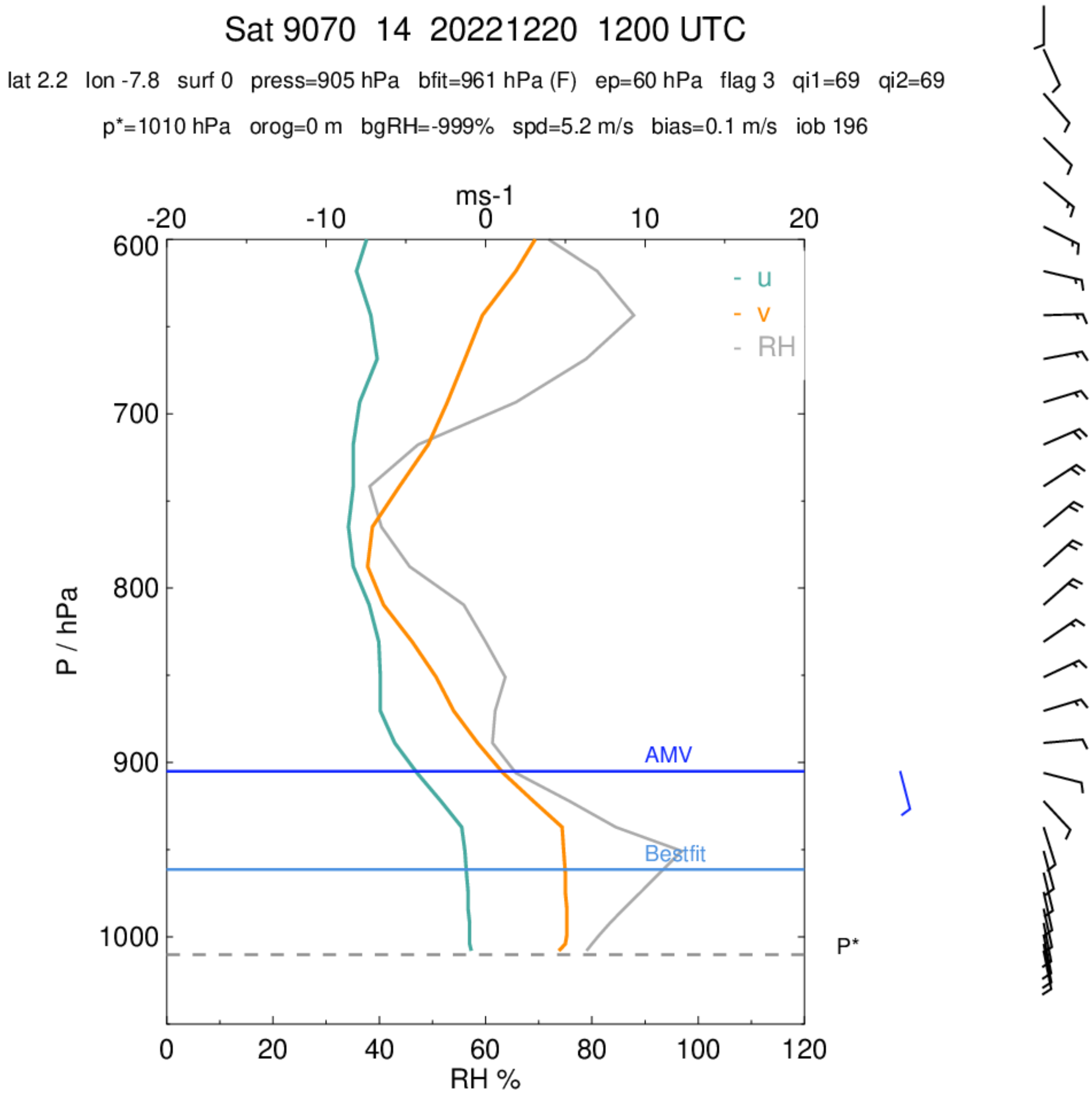

Figure 24. 11:45 UTC on 20/12/2022. Model guess vertical profile at the location of the AMV in the top left of Figure 22: u-wind component (green), v-wind (orange), and relative humidity (grey). The reported AMV pressure is shown by the dark blue horizontal line, the model best-fit pressure by the light blue line.. A profile of model wind barbs is shown to the right of the plot, alongside the AMV wind barb in dark blue. There is a change in direction where the humidity drops at the top of the boundary layer.

A plot of the reported NWC SAF AMV heights below 850 hPa is shown in Figure 25.

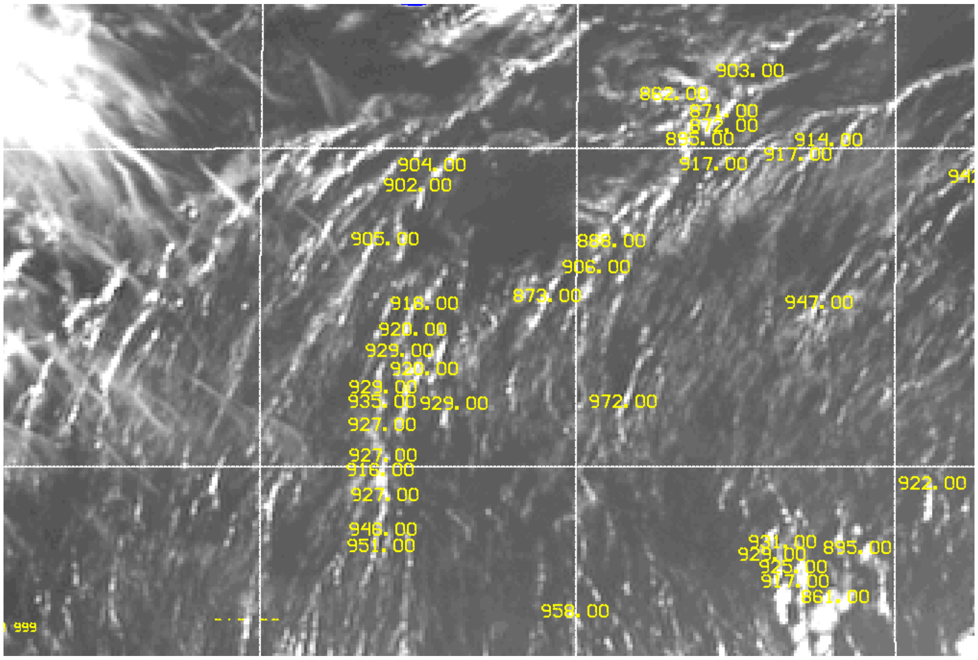

Figure 25. 11:45 UTC on 20/12/2022. Assigned NWC SAF AMV heights below 850 hPa in yellow.

What has been found:

1. There are large differences in AMV directions and model guess. The AMVs agree with surface wind direction from the scatterometer winds (Figure 22).

2. The movie and Figure 23 support that boundary layer clouds are moving north in the same direction as the AMVs.

3. The model guess vertical profile shows the height of the top of the boundary layer which is below the AMV height.

4. Most of the AMV reported heights in Figure 25 are around 925 hPa and consistent with being above the top of the boundary layer.

These results suggest that AMVs with heights near the boundary are too high, this is consistent with other studies (Feature 8.1 of AR8), (Santek ,2023), (Lean,2021).

7. Summary

This paper marks the tenth iteration of analysis reports for the NWP SAF AMV monitoring. The status of existing features identified in the monitoring has not significantly changed in the past two years.

Since the last NWP SAF report EUMETSAT, NOAA and JMA have rearranged their prime satellites. GOES-18 has replaced GOES-17, Himawari-9 replaced Himawari-8, Meteosat-9 replaced Meteosat-8 (IODC), and Meteosat-10 replaced Meteosat-11 at 0 degrees East.

Examples of the cross-correlation matrices were shown with various cases studies and it is suggested that the AMV providers, based on a study (Kelly 2021), make more use of these cross-correlation surfaces during their AMV processing.

A new Feature 10.1 was added. It was found during August that the O-B standard deviation from the monthly upper-level monitoring in the tropical African region is much greater than in March. August is the season of organized convection and there are strong outflow regions at the tops of the convection. The upper-level flow, as captured by the AMVs, shows a strongly divergent wind pattern ahead of the MCS. In the case studied in this report, the NWP model completely failed to capture this feature. In these regions the large O-B values suggest the model guesses may often be less reliable.

The second case study shows an example where AMVs derived from clouds in the boundary layer are assigned heights above the boundary layer. This is consistent with Feature 8.1 of AR8 and other studies (Santek 2023 and Lean 2021).

It is hoped the findings of this report will be useful to AMV producers seeking to improve aspects of the AMV derivation schemes, as well as for NWP centres in improving their methods of AMV data assimilation.

Feedback on the cases investigated in this report is welcome via the NWP SAF helpdesk or directly to graeme.a.kelly@metoffice.gov.uk.

8. Acknowledgements

ECMWF statistics are routinely provided thanks to Mohamed Dahoui.

Thanks to James Cotton and Graeme Kelly for routinely generating the monthly monitoring plots and maintaining the AMV section of the NWP SAF website.

All EUMETSAT satellite images are copyright © EUMETSAT and are sourced from the EUMETSAT Data Centre:

http://www.eumetsat.int/website/home/Data/DataDelivery/EUMETSATDataCentre/index.html

9. References

AR8 - Warrick, F., Cotton, J., (2018). NWP SAF AMV monitoring: the 8th Analysis Report (AR8). Document NWPSAF-MO-TR-035. Available from

https://www.nwpsaf.eu/site/monitoring/winds-quality-evaluation/amv/amv-analysis-reports/

Borde, R., Carranza, M., Hautecoeur, O., Barbieux, K. (2019). Winds of Change for Future Operational AMV at EUMETSAT. Remote Sens. 2019, **11**(18), 2111.

EUMETSAT, 2019. Document: EUMETSAT Product History: 1995-2015, EUM/USC/STD/16/853620 v1A, 31 October 2019. Available from

https://www.eumetsat.int/

García-Pereda, J., 2013a: Algorithm Theoretical Basis Document for ‘‘high resolution winds’’ (HRW - PGE09 v3.2). NWC SAF Doc. SAF/NWC/CDOP/INM/SCI/ATBD/09, Issue 3, Rev. 2, 56 pp. [Available online at http://www.nwcsaf.org/scidocs/Documentation/ SAF-NWC-CDOP-INM-SCI-ATBD-09_v3.2.pdf.]

——, 2013b: Validation report for ‘‘high resolution winds’’ (HRW – PGE09 v3.2). NWC SAF Doc. SAF/NWC/CDOP/ INM/SCI/VR/10, Issue 1, Revision 0, 33 pp. [Available online at http://www.nwcsaf.org/scidocs/Documentation/SAF-NWCCDOP-INM-SCI-VR-10_v1.0.pdf

Kelly G A and Pereda J G. (2021) AMV Cross Correlation Matrices

15th International Winds Workshop (wisc.edu)

Katie Lean and Niels Bormann (2021) Using model cloud information to reassign low level AMVs for NWP. Available online at https://www.ecmwf.int/en/elibrary/81223-using-model-cloud-information-reassign-low-level-amvs-nwp.

M Milan, B Macpherson, R Tubbs, Graeme Kelly 2020 - Hourly cycling four-dimensional variational data assimilation. Quarterly Journal of the Royal Meteorological Society DOI:10.1002/qj.pp 3737

Santek D, Dworak R, Wanzong S, Rink T, Lukens K, Reiner, S García-Pereda J. NWC SAF Winds Intercomparison Study Report: 2021 Released 2023 Available from https://www.nwcsaf.org/aemetRest/downloadAttachment/6869

W. Hibbard, D. Santek, M-F. Voidrot-Martinez, D. Kamins, and J. Vroom, UNIX and X Windows: the right choice for interactive systems. Preprints, Conf. Interactive Information and Processing Systems for Meteorology, Oceanography, and Hydrology. Anaheim, Amer. Meteor. Soc., 1990, pp. 162–163.